VOLUME 119, NUMBER 32
AUGUST 13, 1997

JOURNAL OF THE AMERICAN CHEMICAL SOCIETY

Probing the Electronic Structure of Metallocarbohedrenes: M_8C_{12} (M = Ti, V, Cr, Zr, Nb)

San Li, Hongbin Wu, and Lai-Sheng Wang*

Contribution from the Department of Physics, Washington State University, Richland, Washington 99352, and Environmental Molecular Sciences Laboratory, Pacific Northwest National Laboratory, MS K8-88, P.O. Box 999, Richland, Washington 99352

Received March 31, 1997[⊗]

Abstract: We report a systematic study of the electronic structure of the five metcars in the title using anion photoelectron spectroscopy. The electron affinities of the metcars are measured and are found to be metal dependent and increase from Ti_8C_{12} to Cr_8C_{12}. The electronic structures of Zr_8C_{12} and Nb_8C_{12} are found to be similar to Ti_8C_{12} and V_8C_{12}, respectively. All the spectra can be qualitatively interpreted by the molecular orbital schemes derived from a tetracapped tetrahedral M_8C_{12} cluster. This work provides yet the most quantitative electronic and spectroscopic information about the metcars, as well as evidence supporting the tetrahedral structure for the metcars.

Introduction

The discovery of C_{60} in mass spectra of laser vaporization experiments and its subsequent bulk synthesis have spawned a new interdisciplinary field of fullerene research between chemistry and materials science.[1] Therefore, the observation of a special positively charged titanium carbide cluster containing eight Ti and twelve C atoms ($Ti_8C_{12}^+$) in a similar laser vaporization experiment 4 years ago has stimulated a broad scientific interest.[2] A dodecahedral structure with T_h point group symmetry was proposed to account for the stability of this newly found carbide cluster that was named metallocarbohedrene (metcar). The special nature of the $M_8C_{12}^+$ clusters in mass spectra of laser vaporization experiments has been found for several early transition metals including Ti, V, Cr, Fe, Zr, Nb, Mo, and Hf, with $Ti_8C_{12}^+$ being the most prototypical.[2,3]

However, despite extensive theoretical[4−8] and experimental effort,[9−12] the structure and bonding of the metcars still remains a central unresolved question.[13,14] The original cage structure is highly idealized, and several theoretical calculations have shown alternative structures that are much more stable.[5−8] But the validity of these calculations has not been fully tested due to the lack of quantitative spectroscopic data. Recently, we have obtained the first anion photoelectron spectra of the Ti_8C_{12} metcar.[14] The experiment provided unique electronic and spectroscopic information on the prototypical metcar and revealed a surprisingly low electron affinity (EA) for the Ti_8C_{12} cluster. The photoelectron spectra were interpreted by using theoretical results based on a tetrahedral Ti_8C_{12} cluster (T_d) that has been shown to be the most stable among the many structures calculated.[6−8] However, questions remain about the other metcars. If all the metcars have the same atomic structure as suggested, do they all have similar electronic structure as well? Do they all have very low EAs, as does Ti_8C_{12}? What determines the EA and the electronic structure of the metcars? Can the same electronic structure information obtained theoretically for the T_d structure describe all the metcars? Answers to these questions are critical for understanding the structures and

[⊗] Abstract published in *Advance ACS Abstracts,* August 1, 1997.

(1) Kroto, H.; Heath, J. R.; O'Brien, S. C.; Curl, R. F.; Smalley, R. E. *Nature* **1985**, *318*, 1662−1663. Kratschmer, W.; Lamb, L. D.; Fostiropoulos, K.; Huffman, D. R. *Nature* **1990**, *347*, 354−356.

(2) Guo, B. C; Kerns, K. P.; Castleman, A. W., Jr. *Science* **1992**, *255*, 1411−1413.

(3) Guo, B. C.; Wei, S.; Purnell, J.; Buzza, S.; Castleman, A. W., Jr. *Science* **1992**, *256*, 515−516. Pilgrim, J. S.; Duncan, M. A. *J. Am. Chem. Soc.* **1993**, *115*, 6958−6961.

S0002-7863(97)01015-9 CCC: $14.00

chemical bonding of the metcars and establishing the metcars as a new class of stable molecular clusters.

In this paper, we present a systematic study of all the metcars including Ti, V, Cr, Zr, and Nb using anion photoelectron spectroscopy (PES). PES has proven to be a powerful experimental technique for probing the electronic structure of metal clusters.[15] We show that while the EAs of the metcars do depend on the metals (increasing from left to right in the 3d transition series and decreasing from 3d to 4d transition metals), the basic PES spectra of all the metcars can be interpreted by the molecular orbital schemes derived from the T_d structure, lending credence to the validity of this structure for the metcars. More importantly, the obtained electronic and spectroscopic information can be used quantitatively to compare and verify future theoretical calculations. Direct simulations of the present PES spectra similar to those performed for small silicon and copper clusters should allow the metcar structures to be uniquely and definitively determined.[16]

Experimental Section

The experiments are performed with an apparatus that couples a laser vaporization cluster source and a magnetic-bottle time-of-flight photoelectron analyzer.[17] Clusters formed in the laser vaporization cluster source, containing both neutral and charged species, undergo a supersonic expansion, and are skimmed to form a collimated cluster beam. The negative clusters are extracted perpendicularly from the beam into a time-of-flight mass spectrometer. The mass-selected $M_8C_{12}^-$ clusters are decelerated before being detached by a laser beam from either a Q-switched Nd:YAG laser (3.49 and 4.66 eV) or an ArF excimer laser (6.42 eV). The photoelectrons are collected and analyzed by the magnetic-bottle photoelectron analyzer and calibrated by the known spectra of Cu^- to obtain the electron binding energy spectra.

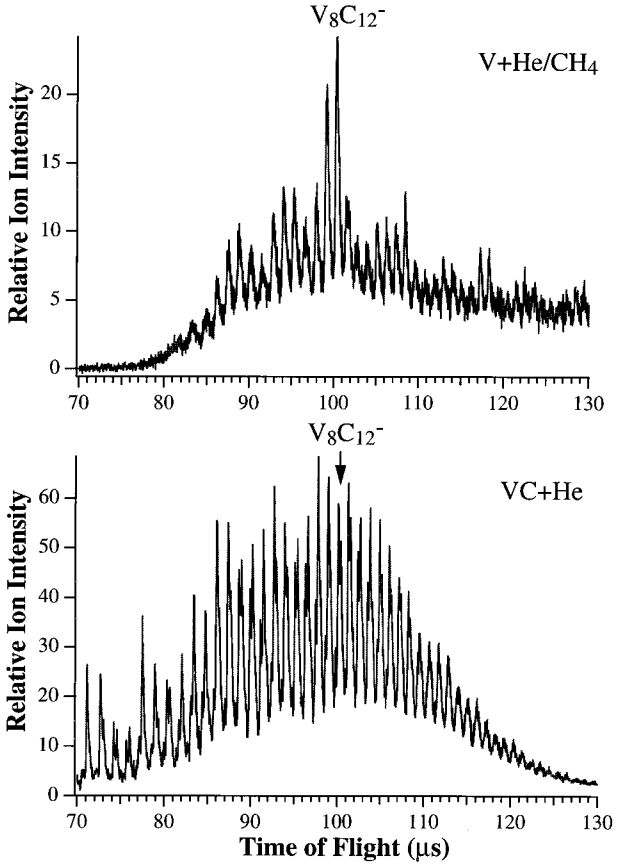

Figure 1. Anion mass spectra of $V_xC_y^-$ clusters produced by two methods: (top) laser vaporization of a pure V target with a He carrier gas seeded with 5% CH_4; (bottom) laser vaporization of a pure VC target with neat He carrier gas. Note the magic peak for the $V_8C_{12}^-$ metcar in the top panel.

Two methods are used to produce the desired $M_8C_{12}^-$ clusters: (1) direct laser vaporization of a pure metal carbide target with neat helium carrier gas and (2) laser vaporization of a pure metal target with helium carrier gas seeded with 5% CH_4. The metcars (positive ions) were discovered with the latter technique in which the $M_xC_y^+$ carbide clusters are formed through a series of complicated dehydrogenation reactions in the laser-induced plasma.[2,3] As pointed out previously,[14] this technique does not produce $Ti_8C_{12}^-$. Presently, we find the same is true for $Zr_8C_{12}^-$. However, this technique does produce $V_8C_{12}^-$, $Cr_8C_{12}^-$, and $Nb_8C_{12}^-$, even with enhanced abundance (magic behavior), as shown in Figures 1−3 (top panel), respectively. The anomalous behavior of the $Ti_8C_{12}^-$ and $Zr_8C_{12}^-$ clusters is not well understood, but may be partly due to the unusually low electron affinities of the

(4) Grimes, R. W.; Gale, J. D. *J. Chem. Soc., Chem. Commun*. **1992**, 1222−1224. Rantala, T. T.; Jelski, D. A.; Bowser, J. R.; Xia, X.; George, T. F. *Z. Phys. D* **1992**, *26*, S255−257. Pauling, L. *Proc. Natl. Acad. Sci. U.S.A.* **1992**, *89*, 8175−8176. Lin, Z.; Hall, M. B. *J. Am. Chem. Soc*. **1992**, *114*, 10054−10055. Reddy, B. V.; Khanna, S. N.; Jena, P. *Science* **1992**, *258*, 1640−1643. Methfessel, M.; van Schilfgaarde, M.; Scheffler, M. *Phys. Rev. Lett.* **1993**, *71*, 209−212. Hay, P. J. *J. Phys. Chem.* **1993**, *97*, 3081−3083. Grimes, R. W.; Gale, J. D. *J. Phys. Chem.* **1993**, *97*, 4616−4620. Reddy, B. V.; Khanna, S. N. *J. Phys. Chem.* **1994**, *98*, 9446−9449. Lou, L.; Guo, T.; Nordlander, P.; Smalley, R. E. *J. Chem. Phys.* **1993**, *99*, 5301−5305. Reddy, B. V.; Khanna, S. N. *Chem. Phys. Lett.* **1993**, *209*, 104−108. Lou, L.; Nordlander, P. *Chem. Phys. Lett.* **1994**, *224*, 439−444.

(5) Ceulemans, A.; Fowler, P. W. *J. Chem. Soc., Faraday Trans*. **1992**, *88*, 2797−2798. Rohmer, M.; de Vaal, P.; Benard, M. *J. Am. Chem. Soc*. **1992**, *114*, 9696−9697. Chen, H.; Feyereisen, M.; Long, X. P.; Fitzgerald, G. *Phys. Rev. Lett.* **1993**, *71*, 1732−1735.

(6) Dance, D. *J. Chem. Soc., Chem. Commun*. **1992**, 1779−1780. Rohmer, M.; Benard, M.; Henriet, C.; Bo, C.; Poblet, J. *J. Chem. Soc., Chem. Commun*. **1993**, 1182−1185. Dance, I. *J. Am. Chem. Soc*. **1996**, *118*, 2699−2707.

(7) Lin, Z.; Hall, M. B. *J. Am. Chem. Soc*. **1993**, *115*, 11165−11168.

(8) Rohmer, M.; Benard, M.; Bo, C.; Poblet, J. *J. Am. Chem. Soc*. **1995**, *117*, 508−517. Rohmer, M.; Benard, M.; Bo, C.; Poblet, J. *J. Phys. Chem.* **1995**, *99*, 16913−16924.

(9) Wei, S.; Guo, B. C.; Purnell, J.; Buzza, S.; Castleman, A. W., Jr. *J. Phys. Chem.* **1992**, *96*, 4166−4170; **1993**, *97*, 9559−9561. Cartier, S. F.; May, B. D.; Toleno, B. J.; Purnell, J.; Wei, S.; Castleman, A. W., Jr. *Chem. Phys. Lett.* **1994**, *220*, 23−28. May, B. D.; Cartier, S. F.; Castleman, A. W., Jr. *Chem. Phys. Lett.* **1995**, *242*, 265−271. Wei, S.; Guo, B. C.; Deng, H. T.; Purnell, J.; Buzza, S.; Castleman, A. W., Jr. *J. Am. Chem. Soc*. **1994**, *116*, 4475−4480. Cartier, S. F.; May, B. D.; Castleman, A. W., Jr. *J. Am. Chem. Soc.* **1994**, *116*, 5295−5299. Cartier, S. F.; May, B. D.; Castleman, A. W., Jr. *J. Chem. Phys.* **1994**, *100*, 5384−5389. Kerns, K. P.; Guo, B. C.; Deng, H. T.; Castleman, A. W., Jr. *J. Chem. Phys.* **1994**, *101*, 8529−8534. Cartier, S. F.; May, B. D.; Castleman, A. W., Jr. *J. Chem. Phys.* **1996**, *104*, 3423−3427. Cartier, S. F.; May, B. D.; Castleman, A. W., Jr. *J. Phys. Chem.* **1996**, *100*, 8175−8180.

(10) Guo, B. C.; Kerns, K. P.; Castleman, A. W., Jr. *J. Am. Chem. Soc*. **1993**, *115*, 7415−7419. Kerns, K. P.; Guo, B. C.; Deng, H. T.; Castleman, A. W., Jr. *J. Am. Chem. Soc.* **1995**, *117*, 4026−4627. Deng, H. T.; Kerns, K. P.; Castleman, A. W., Jr. *J. Am. Chem. Soc.* **1996**, *118*, 446−451. Deng, H. T.; Guo, B. C.; Kerns, K. P.; Castleman, A. W., Jr. *J. Phys. Chem.* **1994**, *98*, 13373−13379.

(11) Byun, Y. G.; Lee, S. A.; Freiser, B. S. *J. Am. Chem. Soc.* **1996**, *100*, 14281−14288. Yeh, C. S.; Afzaal, S.; Lee, S. A.; Byun, Y. G.; Freiser, B. S. *J. Am. Chem. Soc*. **1994**, *116*, 8806−8807. Byun, Y. G.; Freiser, B. S. *J. Am. Chem. Soc.* **1996**, *118*, 3681−3685.

(12) Pilgrim, J. S.; Duncan, M. A. *J. Am. Chem. Soc*. **1993**, *115*, 4395−4396, 9724−9727. Pilgrim, J. S.; Duncan, M. A. *Int. J. Mass Spectrom. Ion Processes* **1994**, *138*, 283−296. Pilgrim, J. S.; Brock, L. R.; Duncan, M. A. *J. Phys. Chem*. **1995**, *99*, 544−550. Brock, L. R.; Duncan, M. A. *J. Phys. Chem.* **1996**, *100*, 5654−5659.

(13) Lee, S.; Gotts, N. G.; von Helden, G.; Bowers, M. T. *Science* **1995**, *267*, 999−1001.

(14) Wang, L. S.; Li, S.; Wu, H. *J. Phys. Chem*. **1996**, *100*, 19211−19214.

(15) Wu, H.; Desai, S. R.; Wang, L. S. *Phys. Rev. Lett*. **1996**, *76*, 212−215; **1996**, *77*, 2436−2439.

(16) Binggeli, N.; Chelikowsky, J. R. *Phys. Rev. Lett.* **1995**, *75*, 493−4936. Massobrio, C.; Pasquarello, A.; Car, R. *Phys. Rev. Lett.* **1995**, *75*, 2104−2107.

(17) Wang, L. S.; Cheng, H.; Fan, J. *J. Chem. Phys.* **1995**, *102*, 9480−9493.

(18) Yang, S.; Taylor, K. J.; Craycraft, M. J.; Conceicao, J.; Pettiette, C. L.; Cheshnovsky, O.; Smalley, R. E. *Chem. Phys. Lett*. **1988**, *144*, 431−436.

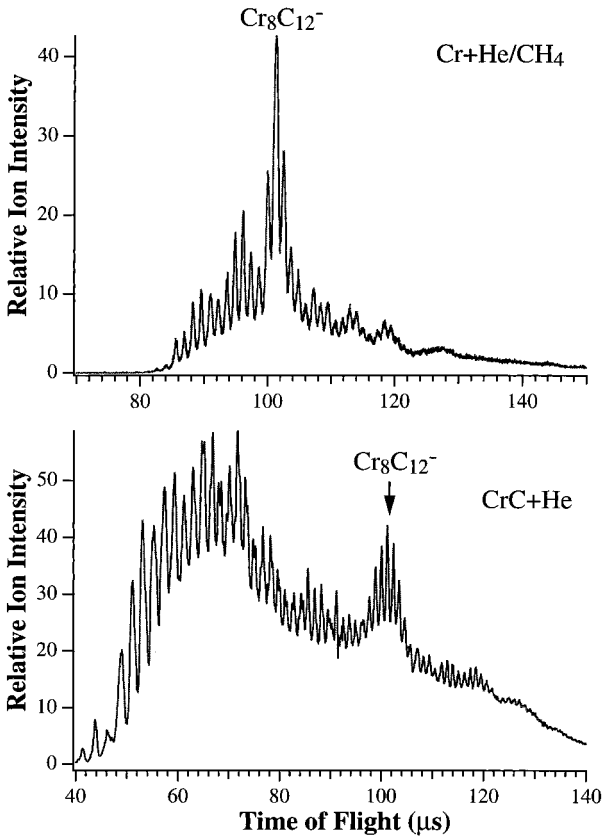

Figure 2. Anion mass spectra of $Cr_xC_y^-$ clusters produced by two methods: (top) laser vaporization of a pure Cr target with a He carrier gas seeded with 5% CH_4; (bottom) laser vaporization of a pure CrC target with neat He carrier gas. Note the magic peak for the $Cr_8C_{12}^-$ metcar in both mass spectra.

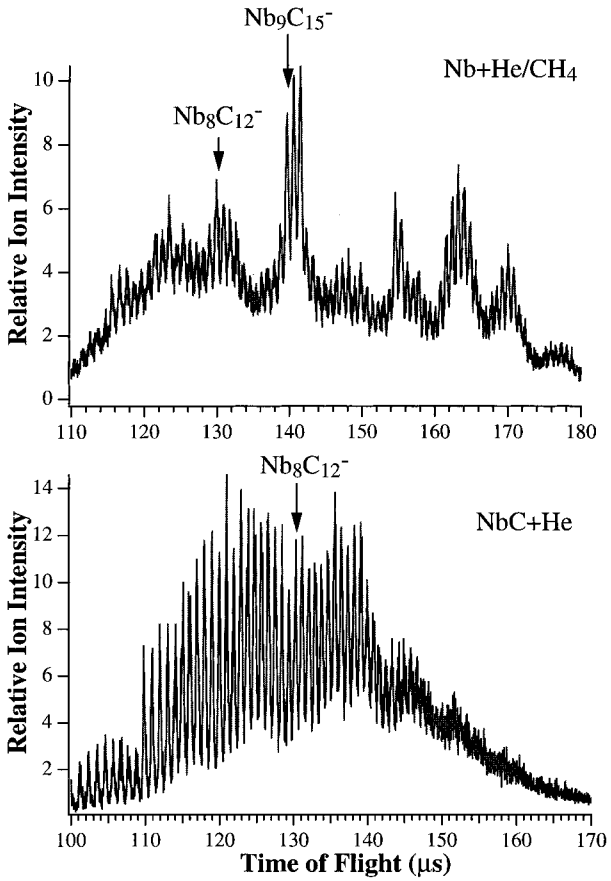

Figure 3. Anion mass spectra of $Nb_xC_y^-$ clusters produced by two methods: (top) laser vaporization of a pure Nb target with a He carrier gas seeded with 5% CH_4; (bottom) laser vaporization of a pure NbC target with neat He carrier gas. Note the slight magic peak for the $Nb_8C_{12}^-$ metcar in the top panel.

corresponding neutral clusters as we have shown. On the other hand, we find that all the $M_8C_{12}^-$ anions, including M = Ti and Zr, can be produced with the first technique by using the pure carbide targets. However, the metcar anions do not show magic behavior when produced in this technique, except for $Cr_8C_{12}^-$, as shown in Figures 1−3 (bottom panel), where the anions produced from both techniques are compared for $V_8C_{12}^-$, $Cr_8C_{12}^-$, and $Nb_8C_{12}^-$. We have measured photoelectron spectra for $V_8C_{12}^-$, $Nb_8C_{12}^-$, and $Cr_8C_{12}^-$ with both techniques and obtained identical spectra.

Results

Figure 4 shows the photoelectron spectra of all five $M_8C_{12}^-$ (M = Ti, V, Cr, Zr, and Nb) clusters at 4.66 eV photon energy. Due to the natural isotope distribution of Zr, the $Zr_8C_{12}^-$ mass peak cannot be fully separated from that of $Zr_8C_{11}^-$ and $Zr_8C_{13}^-$ and the photoelectron spectra of $Zr_8C_{12}^-$ are slightly contaminated. For $Ti_8C_{12}^-$ and $V_8C_{12}^-$, PES spectra were also taken at 193 nm, as shown in Figure 5.

These photoelectron spectra represent transitions between the ground state of the $M_8C_{12}^-$ anions and the ground and excited states of the M_8C_{12} neutrals, governed by the Franck−Condon principle. Or they may be viewed as representations of the occupied molecular orbitals of the $M_8C_{12}^-$ anions in a single-particle approximation. The detachment threshold (the lowest electron binding energy feature) yields the adiabatic EA of the clusters (Table 1). The $Ti_8C_{12}^-$ spectrum yields a very low EA (1.05 eV, lower than the EA of either Ti_8 [ref 15] or C_{12} [ref. 18]) with a rather sharp threshold feature. There is a broad band between about 2.4 and 3.2 eV, followed by more features which are revealed in the 6.42 eV spectrum (Figure 5). The $V_8C_{12}^-$ spectrum (Figure 4) shows a broader threshold band with a higher EA compared to the $Ti_8C_{12}^-$ spectrum. There is a hint of more features at higher binding energies, and these are revealed in the 6.42 eV spectrum (Figure 5), which shows a second band around 4 eV and hints at more features at even higher binding energies. The $Cr_8C_{12}^-$ spectrum displays a very high EA and an even broader threshold band.

The 4d Zr and Nb atoms have similar electronic structure to the 3d Ti and V, respectively, and the electronic structures of the 4d M_8C_{12} clusters are also expected to exhibit similarity to their 3d congeners. Indeed, the $Zr_8C_{12}^-$ spectrum is quite similar to that of $Ti_8C_{12}^-$, also with a very low EA, even though the $Zr_8C_{12}^-$ spectrum is slightly contaminated by other species. As shown previously for the photoelectron spectra of $Ti_8C_y^-$ (y = 10−14), the Ti_8C_{12} metcar has the lowest EA among the series.[14] We expect that the $Zr_8C_y^-$ series should show similar behavior, and thus the EA measured from Figure 5 for Zr_8C_{12} should not be affected by the slight contamination from $Zr_8C_{11}^-$ and $Zr_8C_{13}^-$. The $Nb_8C_{12}^-$ spectrum is interesting, showing a sharp threshold feature followed by a broad band. It yields an EA value for Nb_8C_{12} very similar to that of V_8C_{12} (Table 1).

Discussion

Electronic Structure of the M_8C_{12} Metcars (M = Ti, V, Cr, Zr, and Nb). The photoelectron spectra shown in Figure 4 for the $M_8C_{12}^-$ clusters are the most direct experimental representations of the electronic structures of these clusters. Understanding and correct interpretation of these spectra can provide information about the electronic properties of the metcars, as well as insight into their chemical and structural properties. Among the many theoretical calculations performed

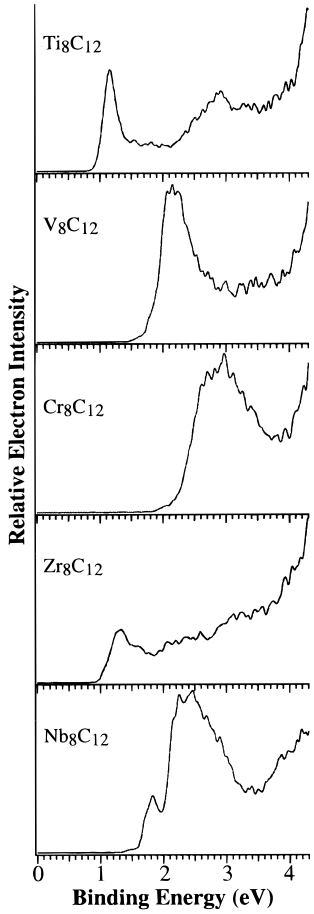

Figure 4. Photoelectron spectra of $Ti_8C_{12}^-$, $V_8C_{12}^-$, $Cr_8C_{12}^-$, $Zr_8C_{12}^-$, and $Nb_8C_{12}^-$ at 4.66 eV photon energy.

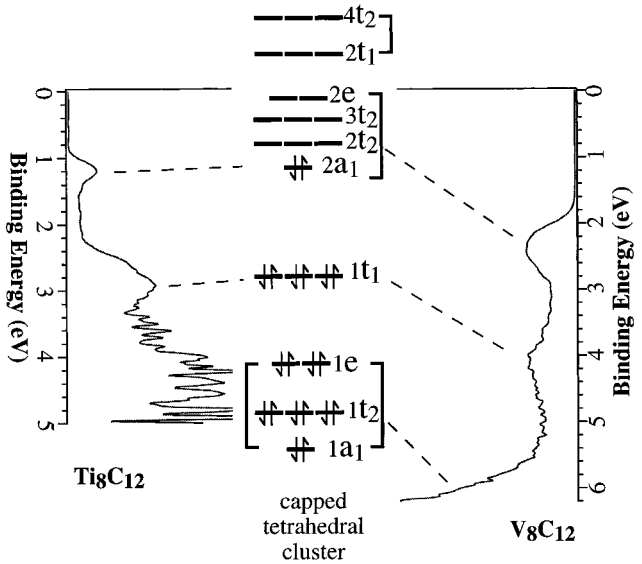

Figure 5. Photoelectron spectra of $Ti_8C_{12}^-$ and $V_8C_{12}^-$ at 6.42 eV photon energy, compared with the valence molecular orbitals derived from the tetracapped tetrahedral M_8C_{12} metcar (from ref 7). The occupation is for Ti_8C_{12}. For V_8C_{12} and Cr_8C_{12}, more orbitals above the $2a_1$ orbital will be successively occupied.

so far on the metcars, the most stable structure has been found not to be the idealized T_h structure. Indeed, several lower symmetry structures are found to be much more stable than the T_h structure.[5−8] Among the lower symmetry structures, the one with a tetrahedral symmetry (T_d) has been predicted to have the lowest energy[6−8] and is shown schematically in Figure 6 along with the T_h structure. The T_d structure has been studied

Table 1. Adiabatic Electron Affinities of the M_8C_{12} Metcars (M = Ti, V, Cr, Zr, and Nb)[a]

Ti_8C_{12}	V_8C_{12}	Cr_8C_{12}	Zr_8C_{12}	Nb_8C_{12}
1.05(0.05)	1.80(0.08)	2.28(0.08)	1.02(0.06)	1.65(0.06)

[a] All the electron affinities are measured from the 3.49-eV spectra since the instrumental resolution is better at 3.49 eV photon energy. Due to the lack of resolved vibrational features, the electron affinity is determined by drawing a straight line at the leading edge of the spectrum and taking the intercept with the binding energy axis plus a constant of 0.05 eV to account for the instrumental resolution and a finite thermal effect. The larger uncertainties are due to the lack of a sharp onset in the spectra.

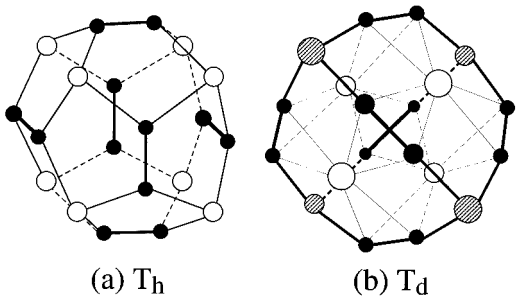

Figure 6. Schematic drawings of the dodecahedral T_h M_8C_{12} metcar and the tetracapped tetrahedral M_8C_{12} cluster calculated to be of the lowest energy among the different M_8C_{12} isomers.

more extensively, and detailed orbital interactions and distinct valence molecular orbital (MO) schemes have been predicted.[6−8] The original T_h structure can be viewed as a cubic M_8 framework with six C_2 units capping the six cube faces. There is little metal−metal interaction because of the large M−M distances. The T_d structure can be envisioned by distorting the cubic M_8 framework and rotating the six C_2 units to be along the diagonals of the faces. Consequently, the eight metal atoms form a tetracapped tetrahedral M_8 cluster with the six C_2 units aligning along the six edges formed by the four capping M atoms (shaded circle in Figure 6b). In the T_d structure, both the M−C interactions and M−M interactions are optimized: each C_2 unit, which can be viewed as an acetylene-like unit (C_2^{2-}), is σ-bonded to two capping M atoms and π-bonded to two M atoms forming the inner tetrahedron (open circles) as indicated by the thin lines in Figure 6b. Each metal atom is left with three d orbitals for the metal−metal interactions that form the valence orbitals of the metcars. Figure 5 shows the MO scheme for these interactions, compared with the PES spectra of $Ti_8C_{12}^-$ and $V_8C_{12}^-$. In the single particle approximation, features in the PES spectra can be attributed to specific occupied MOs.

The valence electrons of the eight metal atoms, except 12 that are donated to the 6 C_2 units, are expected to fill these orbitals, which are grouped into four groups, ($1a_1$, $1t_2$, 1e), ($1t_1$), ($2a_1$, $2t_2$, $3t_2$, 2e), and ($2t_1$, $4t_2$). Figure 5 shows the occupation of the Ti_8C_{12} cluster, which fills up to the $2a_1$ orbital with the remaining 20 valence electrons on the Ti atoms (32 minus 12). The filling of the 9 bonding orbitals from $1a_1$ to $1t_1$ is expected to make an especially stable cluster. It has been suggested that the dication $[Ti_8C_{12}]^{2+}$, which fills just the 9 bonding orbitals, might be specially stable and may be the best target for synthesis in bulk form.[7] In the anion, the $2t_2$ orbital will be singly occupied. It is seen that the three groups of occupied MOs correspond nicely to the three bands in the PES spectrum of $Ti_8C_{12}^-$.

If V_8C_{12} has the same T_d structure, the same orbital scheme should apply. With eight more electrons in V_8C_{12} than in Ti_8C_{12}, more orbitals are expected to be filled. The PES spectra of $V_8C_{12}^-$ should exhibit a similar pattern to that of $Ti_8C_{12}^-$, as dictated by the same orbital scheme. Due to the increased

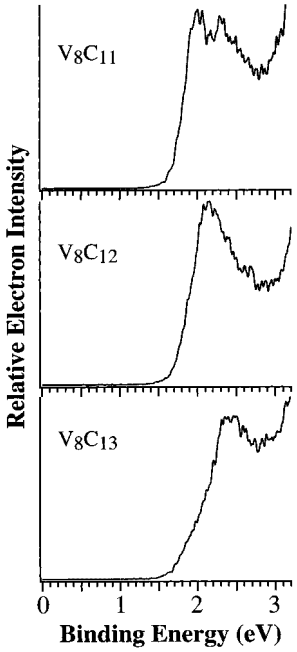

Figure 7. Photoelectron spectra of $V_8C_{11}^-$, $V_8C_{12}^-$, and $V_8C_{13}^-$ at 3.49 eV photon energy.

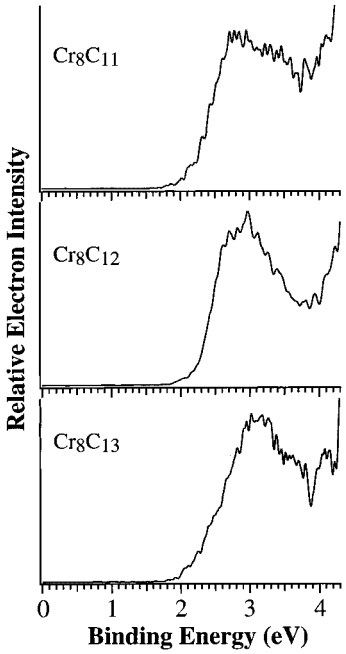

Figure 8. Photoelectron spectra of $Cr_8C_{11}^-$, $Cr_8C_{12}^-$, and $Cr_8C_{13}^-$ at 4.66 eV photon energy.

EA of V_8C_{12}, the 4.66 eV spectrum of $V_8C_{12}^-$ (Figure 4) only reveals one full broad band. However, the 6.42 eV spectrum of $V_8C_{12}^-$ (Figure 5) reveals more features that bear apparent similarities to that of $Ti_8C_{12}^-$ and indeed can be interpreted by the same orbital scheme as shown. The broader first band in the $V_8C_{12}^-$ spectra reflects consistently the increased occupation of the third group of orbitals. The higher EA of V_8C_{12} can be understood to be due to the increased nuclear charge in V compared to Ti.

Similarly, the Cr_8C_{12} cluster with the same T_d symmetry will fill up the third group of MOs to the 2e orbital, making a closed shell electron configuration. In the $Cr_8C_{12}^-$ anion, the extra electron should enter the $2t_1$ orbital. However, only one broad band may result if the splitting between the $2t_1$ (LUMO) and 2e (HOMO) orbitals is not too big. This seems to be consistent with the very broad band observed for the $Cr_8C_{12}^-$ metcar. Again, its very high EA can be accounted for by the further increased nuclear charge in the Cr atom. It is interesting to note that the $Cr_8C_{12}^-$ anion shows particularly strong magic behavior in the mass spectra (Figure 2). In fact, $Cr_8C_{12}^-$ is the only system that exhibits a magic behavior in the mass spectrum when produced with a pure carbide target (Figure 2, bottom panel). This is consistent with the theoretical prediction based on the T_d structure that suggests special stability for the Cr_8C_{12} cluster because of its closed shell electronic structure.[7] However, the PES spectrum of $Cr_8C_{12}^-$ (Figure 4) shows that the HOMO-LUMO gap must be very small.

For the Zr_8C_{12} and Nb_8C_{12} metcars, the enhanced 4d−4d interactions may induce larger splittings in the basic orbital scheme shown in Figure 5. Nevertheless, their electronic structure should be essentially similar to that of the corresponding 3d congeners. Indeed, the $Zr_8C_{12}^-$ spectrum shows clear similarity to that of $Ti_8C_{12}^-$, and they both yield very low EAs for the neutral clusters. The spectrum of $Nb_8C_{12}^-$ is expected to resemble that of $V_8C_{12}^-$. They both have very similar EAs. The splitting and broader band observed in $Nb_8C_{12}^-$ probably reflect the enhanced 4d−4d interactions.

The unusually low EA of Ti_8C_{12} was interpreted as due to the splitting between the bonding and slightly antibonding orbital sets, i.e., between the $1t_1$ orbital and the ($2a_1$, $2t_2$, $3t_2$, 2e) group

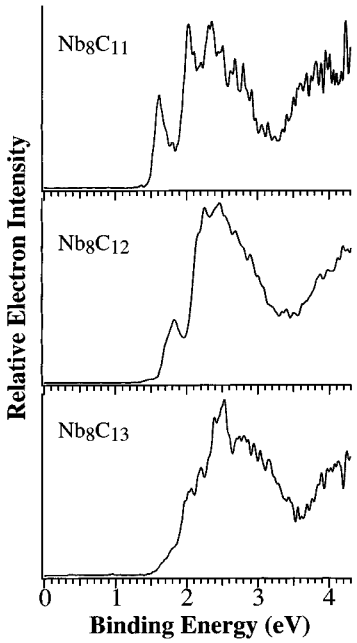

Figure 9. Photoelectron spectra of $Nb_8C_{11}^-$, $Nb_8C_{12}^-$, and $Nb_8C_{13}^-$ at 4.66 eV photon energy.

of orbitals. The splitting between these two sets of orbitals seems to be similar from Ti_8C_{12} to V_8C_{12} as revealed by the similar splitting between the first and second photoemission bands (Figure 5). Therefore, the EA increase from Ti_8C_{12} to Cr_8C_{12} across the 3d series is interpreted to be mostly due to the nuclear charge effect and the poor screening of the 3d electrons. The slightly smaller EAs of the Zr_8C_{12} and Nb_8C_{12} compared to their 3d counterparts are likely due to the enhanced 4d−4d interactions that induce larger splitting among the MOs. This is consistent with the broader widths of their PES features that are probably due to the enhanced splittings among the ($2a_1$, $2t_2$, $3t_2$, 2e) set of orbitals.

All the PES spectra for the metcars show a rather high density of states near the threshold (Fermi level). This is quite different from that of C_{60}^-, whose PES spectrum showed a large energy gap near the threshold.[19] That energy gap is responsible for

the chemical inertness of the C_{60} molecule and the insulating properties of the solid C_{60} fullerite. The high density of low-lying excited states for the metcars is consistent with their considerable chemical reactivity,[10,11] suggesting that the metcars are unlikely to exist as the pure M_8C_{12} molecular form and will need to be passivated.

The current experiments suggest that indeed all the M_8C_{12} metcars seem to have a similar geometrical structure. The special stability of these clusters seems to derive from the unique bonding properties embodied in the cluster structure, rather than the electronic structure, since the different clusters have quite different valence electrons. The electronic structure does play a role as seen from the mass spectra of the $Cr_8C_{12}^-$ cluster (Figure 2). The neutral Cr_8C_{12} cluster is closed shell and was predicted to exhibit particular electronic stability.[7] Indeed, the anion mass spectra of $Cr_8C_{12}^-$ are quite special, in particular, it is the only system that exhibits a magic peak when pure carbide is used to produce the cluster.

The M_8C_{11} and M_8C_{13} Clusters: Similarity to the M_8C_{12} Cluster. As shown in all the previous positive ion mass spectra, the $M_8C_{11}^+$ and $M_8C_{13}^+$ clusters also exhibit somewhat enhanced abundance. The anion mass spectra (Figures 1−3) also show that the $M_8C_{11}^-$ and $M_8C_{13}^-$ mass peaks are somewhat special, accompanying the magic $M_8C_{12}^-$ mass peak. As we have shown before,[14] the PES spectra of $Ti_8C_{11}^-$ and $Ti_8C_{13}^-$ show some similarity to that of the $Ti_8C_{12}^-$ metcar. Figures 7−9 compare the PES spectra of $M_8C_{11}^-$ and $M_8C_{13}^-$ to that of $M_8C_{12}^-$ for M = V, Cr, and Nb, respectively. There is apparent similarity among these spectra, particularly between the $M_8C_{11}^-$ and $M_8C_{12}^-$ clusters. Ion mobility experiments on $Ti_8C_{11}^+$, $Ti_8C_{12}^+$, and $Ti_8C_{13}^+$ show that they all have similar mobility, i.e., similar molecular shapes.[13] If the T_d structure for the M_8C_{12} metcar is correct, then the M_8C_{11} cluster may be viewed as replacing a C_2 unit in M_8C_{12} with a C atom. Similarly, the M_8C_{13} cluster can be viewed as replacing a C_2 unit in M_8C_{12} with a C_3 unit. C atom, C_2, and C_3 species are expected to be abundant in the plasma where the carbide clusters and the metcars are formed. Therefore, it is probably not too surprising that these clusters with one extra and one less C atom than the ideal metcar composition are also formed with some preference. In any case, these clusters should also be interesting to study since they seem to be intimately related to the M_8C_{12} metcars.

(19) Wang, L. S.; Alford, J. M.; Chai, Y.; Diener, M.; Zhang, J.; McClure, S. M.; Guo, T.; Scuseria, G. E.; Smalley, R. E. *Chem. Phys. Lett.* **1993**, *207*, 354−359.

Conclusions

We have shown that the anion photoelectron spectra of the five M_8C_{12} metcars (M = Ti, V, Cr, Zr, Nb) can all be interpreted systematically, albeit qualitatively, on the basis of the electronic structure information obtained from the T_d structure. This lends considerable credence to the validity of this structure for the metcars. The photoelectron spectra provide yet the most quantitative electronic structure and spectroscopic data that can be used to compare quantitatively with future theoretical calculations and should allow the metcar structures to be definitively and uniquely determined.

Acknowledgment. We thank Dr. Chuanfan Ding for useful discussions and Mr. Xi Li for experimental assistance. The support of this research by the National Science Foundation through a CAREER Program Award (DMR-9622733) is gratefully acknowledged. The work is performed at Pacific Northwest National Laboratory, operated for the U.S. Department of Energy by Battelle under contract DE-AC06-76RLO 1830.

JA9710159